Talanta 142 (2015) 35–42

Contents lists available at ScienceDirect

Talanta

journal homepage: www.elsevier.com/locate/talanta

Flow-injection amperometric determination of glucose using a biosensor based on immobilization of glucose oxidase onto Au seeds decorated on core Fe_3O_4 nanoparticles

Anchalee Samphao [a,b,*], Preeyanut Butmee [a], Juthamas Jitcharoen [a], Ľubomír Švorc [c], Georg Raber [d], Kurt Kalcher [d]

[a] Department of Chemistry and Center of Excellence for Innovation in Chemistry, Faculty of Science, UbonRatchathani University, UbonRatchathani 34190, Thailand
[b] Department of Chemistry, Faculty of Science, UbonRatchathani University, UbonRatchathani 34190, Thailand
[c] Institute of Analytical Chemistry, Faculty of Chemical and Food Technology, Slovak University of Technology in Bratislava, Radlinského 9, Bratislava SK-812 37, Slovak Republic
[d] Institute of Chemistry-Analytical Chemistry, Karl-Franzens University, A-8010 Graz, Austria

ARTICLE INFO

Article history:
Received 5 November 2014
Received in revised form
27 January 2015
Accepted 28 January 2015
Available online 27 March 2015

Keywords:
Core–shell magnetite gold nanoparticles
Screen-printed electrode
Amperometric biosensor
Glucose
Flow-injection analysis

ABSTRACT

An amperometric biosensor based on chemisorption of glucose oxidase (GOx) on Au seeds decorated on magnetic core Fe_3O_4 nanoparticles (Fe_3O_4@Au) and their immobilization on screen-printed carbon electrode bulk-modified with manganese oxide (SPCE{MnO_2}) was designed for the determination of glucose. The Fe_3O_4@Au/GOx modified SPCE{MnO_2} was used in a flow-injection analysis (FIA) arrangement. The experimental conditions were investigated in amperometric mode with the following optimized parameters: flow rate 1.7 mL min^{-1}, applied potential +0.38 V, phosphate buffer solution (PBS; 0.1 mol L^{-1}, pH 7.0) as carrier and 3.89 unit mm^{-2} enzyme glucose oxidase loading on the active surface of the SPCE. The designed biosensor in FIA arrangement yielded a linear dynamic range for glucose from 0.2 to 9.0 mmol L^{-1} with a sensitivity of 2.52 μA mM^{-1} cm^{-2}, a detection limit of 0.1 mmol L^{-1} and a quantification limit of 0.3 mmol L^{-1}. Moreover, a good repeatability of 2.8% (number of measurements $n=10$) and a sufficient reproducibility of 4.0% (number of sensors $n=3$) were achieved. It was found that the studied system Fe_3O_4@Au facilitated not only a simpler enzyme immobilization but also provided wider linear range. The practical application of the proposed biosensor for FIA quantification of glucose was tested in glucose sirup samples, honeys and energy drinks with the results in good accordance with those obtained by an optical glucose meter and with the contents declared by the producers.

1. Introduction

The development of biosensors has attracted much attention due to their possible applications in the fields of clinical monitoring and diagnosis as well as in industrial quality and process control [1–3]. Very widespread are amperometric enzyme biosensors which are often based on the oxidation of the target analyte with an appropriate oxidase, where the formation of hydrogen peroxide is monitored (first generation oxidase biosensors) [4–6]. Glucose oxidase represents one of the most exploited enzymes of the oxidase group [7]. The fabrication of glucose biosensors was achieved with immobilization of the enzyme by different methods such as physical adsorption [8,9], microencapsulation [10,11], entrapment [12,13], cross-linking [14,15], or covalent bonding [16,17]. However, some of these sensors show only fair sensitivity and stability or have the disadvantage that the immobilization procedures are long and require many steps.

Food production and quality control requires fast and easy-to-manage sensing of certain food components in order to guarantee proper processing. The quicker the analysis can be performed, the better the production process can be altered or adapted. Facile analysis and quick handling can be simply achieved by magnetic nanoparticles.

Nanoparticles of noble metals have attracted much attention recently, particularly because of their high surface area combined with improvements of the electron transfer. Thus, very often catalytic or even synergistic effects with other modifiers can be observed with corresponding electrochemical sensors.

* Corresponding author at: Department of Chemistry and Center of Excellence for Innovation in Chemistry, Faculty of Science, UbonRatchathani University, UbonRatchathani 34190, Thailand. Tel.: +66 85 055 1717; fax: +66 45 288 400.
E-mail address: scanchsa@mail2.ubu.ac.th (A. Samphao).

http://dx.doi.org/10.1016/j.talanta.2015.01.046
0039-9140/

Recently, Fe_3O_4@Au core shell magnetic gold nanoparticles have been widely investigated as great materials for the detection of biomolecules in biosensors due to excellent biocompatibility, magnetic properties, low toxicity, and high stability [18–22]. Fe_3O_4@Au magnetic nanoparticles in biosensors feature many advantages, such as (i) rapid production of the biosensor with the modified nanoparticles under chemically mild conditions using an external magnetic field only, (ii) high surface-to-volume ratio and biocompatibility of Au resulting in increased sensitivity, (iii) less cluster aggregation when Fe_3O_4@Au magnetic nanoparticles are directly used, and (iv) simply renewable surface of the electrode with the aid of an external magnetic field. Moreover, the incorporation of some metal oxides in carbonaceous materials results in an improvement of the biosensor's sensitivity and operation potential. MnO_2 is considered as a promising candidate for many electrochemical applications because it has many user-friendly properties, such as low-cost, easy availability and good chemical stability; it is eco-friendly and can be used in green chemistry [23–27].

The growing interest of using biosensors as quantitative detectors in flow-injection analysis derives from their excellent selectivity, high sensitivity as well as good repeatability and response times in compatibility with flow-injection analysis (FIA). Screen-printed carbon electrodes (SPCE) in combination with FIA have been frequently used for the construction of simple portable devices for fast screening purposes and in-field/on-site monitoring, because of their low cost, high sample throughput and easy integration into mass-production processes [28–30]. Screen-printed electrodes are an ideal type of mass-produced sensors because they show many advantages over other heterogeneous electrodes (e.g., carbon paste), such as easy, quick and reproducible mass-production with equivalent electrode characteristics, high mechanical robustness, long shelf-lifetime and possibility of miniaturization.

This paper describes the construction, characterization and application of a glucose biosensor based on GOx/Fe_3O_4@Au/SPCE{MnO_2} using FIA in amperometric mode. The basic cross-over effects between MnO_2 and Au-NPs should be investigated focusing on easy handling of the sensor in combination with low intensity of labor involved. A synergistic effect of MnO_2 as a mediator in combination with Fe_3O_4 nanoparticles, resulting in an enhanced sensitivity, was observed. Moreover, the practical application of this biosensor in FIA arrangement was successfully manifested by quantifying the glucose content in food samples.

2. Experimental

2.1. Reagents and solutions

Highly pure water (Mili-Q cartridge system, 18.2 MΩ cm) was used throughout for preparing solutions. Glucose oxidase from *Aspergillus niger* (EC 1.1.3.4, specific activity 250 kU/g, GOx) and $HAuCl_4 \cdot 3H_2O$ were purchased from Sigma Aldrich (Austria). All other chemicals were of analytical grade (Sigma Aldrich, Austria) and used without further purification. A permanent neodymium magnet (8 mm in diameter, 3 mm in depth) was purchased from Master Magnetics, Inc. (Castle Rock, China). Phosphate buffer solutions (PBS, 0.1 mol L^{-1}) with different pH values were prepared by mixing solutions of potassium dihydrogen phosphate (0.1 mol L^{-1}) and disodium hydrogen phosphate (0.1 mol L^{-1}). The glucose stock solution (5.55 mol L^{-1}) was prepared by dissolving glucose in water. Energy drinks and glucose sirup were bought in a supermarket in Thailand, honey samples were purchased from local supermarkets in Thailand and Austria. Dilution of working solutions and samples was performed just before analysis with the desired pH phosphate buffer solution.

2.2. Apparatus

The flow-injection system was constructed using a peristaltic pump (ISMATEC, REGLO Analog model MS-2/6, Switzerland), an injection valve (5020 Rheodyn, Cotati, CA, USA), and a thin-layer electrochemical detector (LC 4C, BASi, West Lafayette, Indiana, USA) with a flow through cell (spacer thickness 0.19 mm; CC-5, BASi) in combination with an electrochemical workstation (Auto-Lab, PGSTAT12, Metrohm). The working electrode (screen printed carbon electrode bulk-modified with MnO_2) was placed into the groove of a corresponding Teflon plate which was fixed directly via the spacer to the back plate of the thin layer cell. A cylindrically shaped neodymium magnet was placed into a drilling on the outer side of the Teflon plate, positioned in the center just behind the working electrode. Silver conductive paint (Electrolube Ltd., Wargrave Berkshire, UK) was applied on one end of the SPCE, to which a crocodile clamp was attached for electrical contact; an Ag/AgCl-electrode (3 mol L^{-1} KCl) served as the reference. The steel back plate of the thin layer cell acted as the auxiliary electrode. The pH of solutions was measured with a pH-meter from Sartorius (PP-50, Germany). A glucose meter (FreeStyle Lite Test Strips, Abbott Diabetes Care, USA) was used as a comparative method for analysis of the samples.

2.3. Synthesis of Fe_3O_4@Au seeds nanoparticles

The nanoparticles were prepared as described elsewhere [31–34]. In short, all glassware used for the synthesis was cleaned with aqua regia. Fe_3O_4 nanoparticles (0.0150 g, diameter < 50 nm, Sigma Aldrich) were suspended in 200 mL of water and sonicated for 10–15 min at 0 °C in an ultrasonic bath (Transsonic 700/H, Elma). Au seeds on the Fe_3O_4 cores were prepared by adding $HAuCl_4$ (0.8 mole per mole of Fe_3O_4) and subsequently 0.04 mole $NaHB_4$ to the cooled suspension which was sonicated for further 10–15 min and kept in a refrigerator until use.

2.4. Preparation of the glucose biosensor for flow-injection analysis

Screen-printed electrodes were prepared by mixing manually MnO_2 (0.05 g) and carbon ink (1 g; Electrodag 421 SS, Acheson) for 10–30 min and subsequent sonication for 30 min in the ultrasonic bath. Five percent of MnO_2 is the optimum concentration of the modifier in the ink according to previous studies [23,24,35]. The resulting mixture was printed onto an inert laser pre-etched ceramic support ($113 \times 166 \times 0.635$ mm^3, CLS 641000396R, CoorsTek, Glenrothes, Scotland) by a semi-automatic screen-printing device (SP-200, MPM, Franklin, MA, USA). Thick layers of the modified carbon ink were formed by brushing the ink through an etched stencil (thickness 100 μm, electrode printing area 105 mm^2). The screen printed plates were dried at room temperature overnight before use.

The Fe_3O_4@Au seeds nanoparticles were loaded with the enzyme through adsorption by adding 20 μL of the GOx solution (25 U mL^{-1}) in PBS to 200 μL of the nanoparticle suspension in a vial (1.5 mL micro-centrifuge tube, 616.201, Greiner Labor Technic), mixing with a vortex mixer for 15 min and then left overnight in a refrigerator at 4 °C until use; with exposure times of 8 h or more maximum signal was obtained. The resulting mixture was directly applied onto the active area of the SPCE (≈ 14 mm^2) prior to launching the measurements. The particles were attached to the electrode surface by the magnet of the electrode holder (Fig. 1); the sensor surface was rinsed with water before assembling the thin layer cell.

2.5. Electrochemical measurement

2.5.1. Cyclic voltammetry

Cyclic voltammograms were recorded by batch measurements (10 mL with 0.1 mol L^{-1} KCl as the supporting electrolyte) from an initial potential of −1.0 V to a vertex potential of +1.0 V. The scan rate was 100 mV s^{-1}; usually three cycles were recorded.

2.5.2. Amperometry with FIA

Amperograms were recorded from +0.26 to +0.48 V in increments of 20 mV. Flow-injection analyses were performed at an applied potential of +0.38 V, the flow rate of the pump was 1.7 mL min^{-1}, and the injection volume was 100 μL of 1.5 mmol L^{-1} H_2O_2 and 0.5 mmol L^{-1} glucose solutions.

2.6. Regeneration of biosensor

When the activity of GOx was obviously rather low (after more than one month of operation) the SPCE was renewed by removing the magnet and subsequently flushing the cell with the carrier to remove the particles. Then a new layer of the enzyme-modified particles was attached to the electrode surface as described above.

2.7. Determination of glucose in samples

Amperometric determinations were carried out by the standard addition method. The FIA system was flushed with the carrier and the amperometric measurement was started. After the baseline had reached a constant current value the samples, unspiked

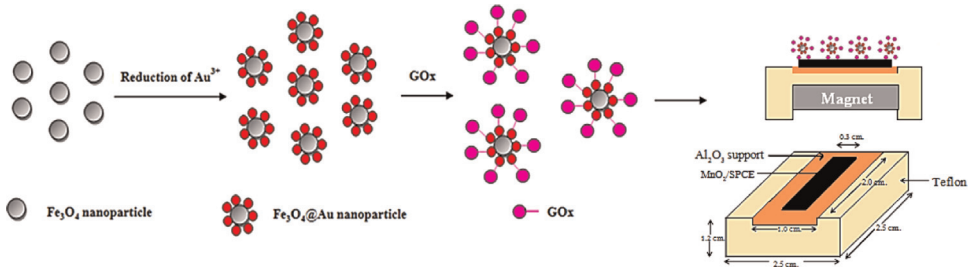

Fig. 1. Schematic presentation of surface coating of Fe_3O_4 nanoparticles with Au seeds, attachment of glucose oxidase and immobilization on a screen printed electrode by the aid of a magnet.

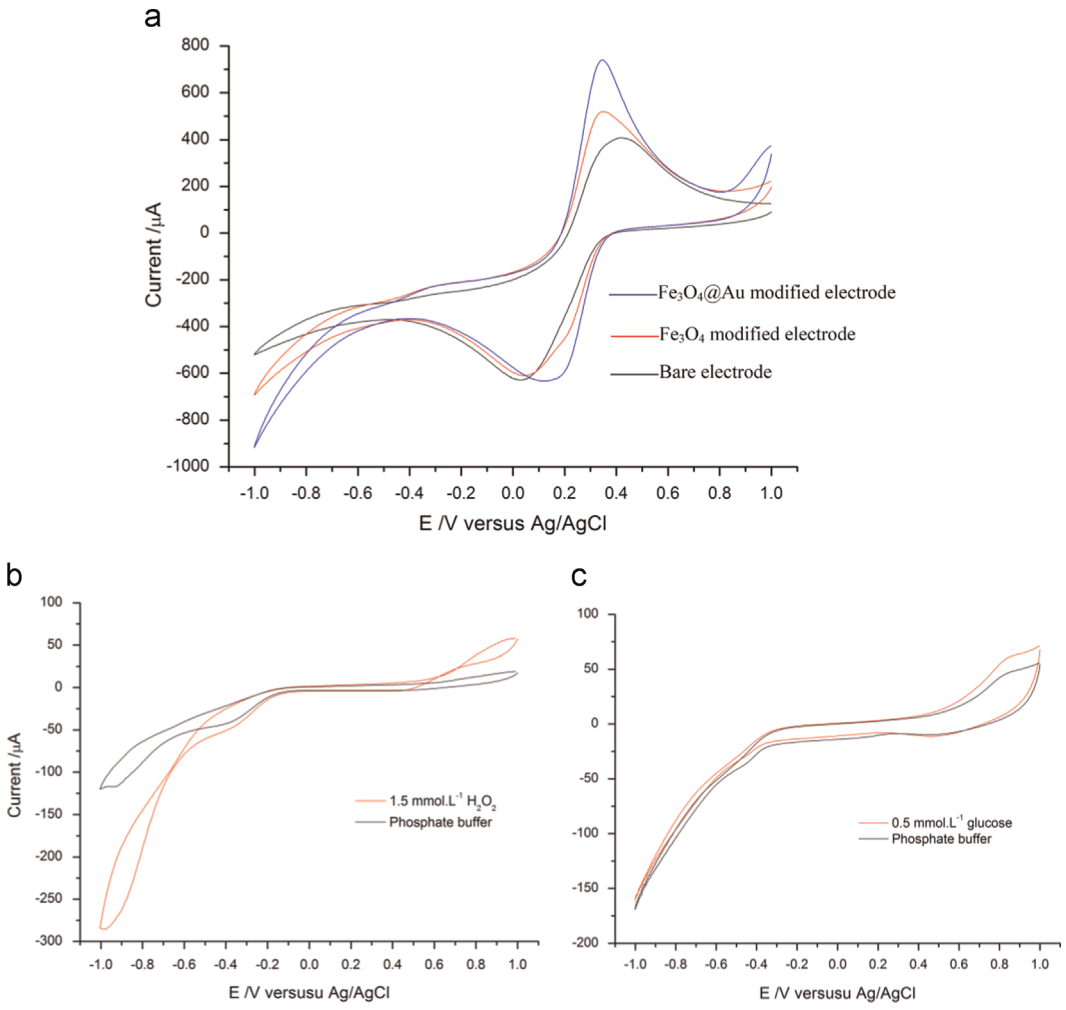

Fig. 2. Cyclic voltammograms of (a) electrodes with 10 mmol L^{-1} $[Fe(CN)_6]^{3-}$; (b) a Fe_3O_4@Au/SPCE{MnO_2} electrode with H_2O_2 (1.5 mmol L^{-1}) and (c) a GOx/Fe_3O_4@Au/SPCE{MnO_2} electrode with glucose (0.5 mmol L^{-1}) in PBS (0.1 mol L^{-1}, pH 7.0).

and spiked, were injected into the carrier solution three times per each solution. The responses were evaluated using the peak heights which were evaluated by tangent fits.

3. Results and discussion

3.1. Electrochemical characterization of the modified electrode

Cyclic voltammetry (CV) was effectively used to characterize the electrochemical properties of the electrode surface using $[Fe(CN)_6]^{3-}$ as a redox probe with 0.1 mol L^{-1} KCl as a supporting electrolyte. The cyclic voltammograms in Fig. 2(a) show that the SPCE modified with Fe_3O_4@Au exhibits the highest magnitude of current response for the redox probe in the anodic range when compared to the bare electrode and to the one modified with naked Fe_3O_4 nanoparticles. This clearly demonstrates the high electroactive effect of designed modifier (Fe_3O_4@Au). Fig. 2(b) shows voltammograms of the SPCE modified with magnetically attached Fe_3O_4@Au measured in the absence (blank) and in the presence of 1.5 mmol L^{-1} H_2O_2 in phosphate buffer solution at pH 7.0. The voltammogram shows significant responses after addition of 1.5 mmol L^{-1} H_2O_2 in both anodic and cathodic ranges which can be assigned to the catalytic oxidation and reduction of hydrogen peroxide, respectively. At positive potentials an evident increase of the oxidation current started from +0.3 V compared to around +0.7 V at the unmodified electrode (not shown). Fig. 2(c) displays the cyclic voltammograms of a SPCE modified with magnetically attached Fe_3O_4@Au/GOx registered in the presence and in the absence of glucose.

Immobilization of GOx was simply achieved by exposition of the suspended Fe_3O_4@Au nanoparticles to the enzyme for 12 h. The procedure is sufficiently long to attach the enzyme to the Au seeds via SH- and/or -S–S-groups of the protein which is known to show a high affinity to bind spontaneously to Au surfaces via chemisorption [34]. Au nanoparticles alone as well as Fe_3O_4@Au seed nanoparticles alone did not show any amperometric response to the target analyte. Naked Fe_3O_4 cores, exposed to a solution of GOx, did not provide any signal due to the fact that they alone are not able to immobilize the enzyme but only in combination with Au seeds. Thus, the results demonstrate that glucose oxidase is sorptively bound to the magnetic nanoparticles in the presence of gold seeds on their surfaces.

In order to improve the current response of the analyte glucose (via the intermediate hydrogen peroxide) synergistic mediators were investigated in FIA mode. Manganese dioxide is known to be very active towards hydrogen peroxide as a mediator lowering its overpotential for oxidation [35]. Therefore, a comparative study was undertaken in order to evaluate the best experimental setup for a respective glucose sensor (Fig. 3a). As expected, glucose oxidase alone, drop-coated onto a screen, resulted in small currents only which even decreased after longer use due to desorption of the enzyme from the sensor surface. Bulk-modification of the thick film carbon electrode improved the situation significantly (1A). MnO_2-modified SPCEs drop-coated with GOx gave initially considerable amperometric responses (3A) which diminished rapidly with time due to desorption of the enzyme whereas the responses of the nanoparticle-modified biosensor in the absence of manganese dioxide were smaller but constant over time (2A). The best results with respect to signal height, repeatability and detection limit were obtained with Fe_3O_4@Au seeds

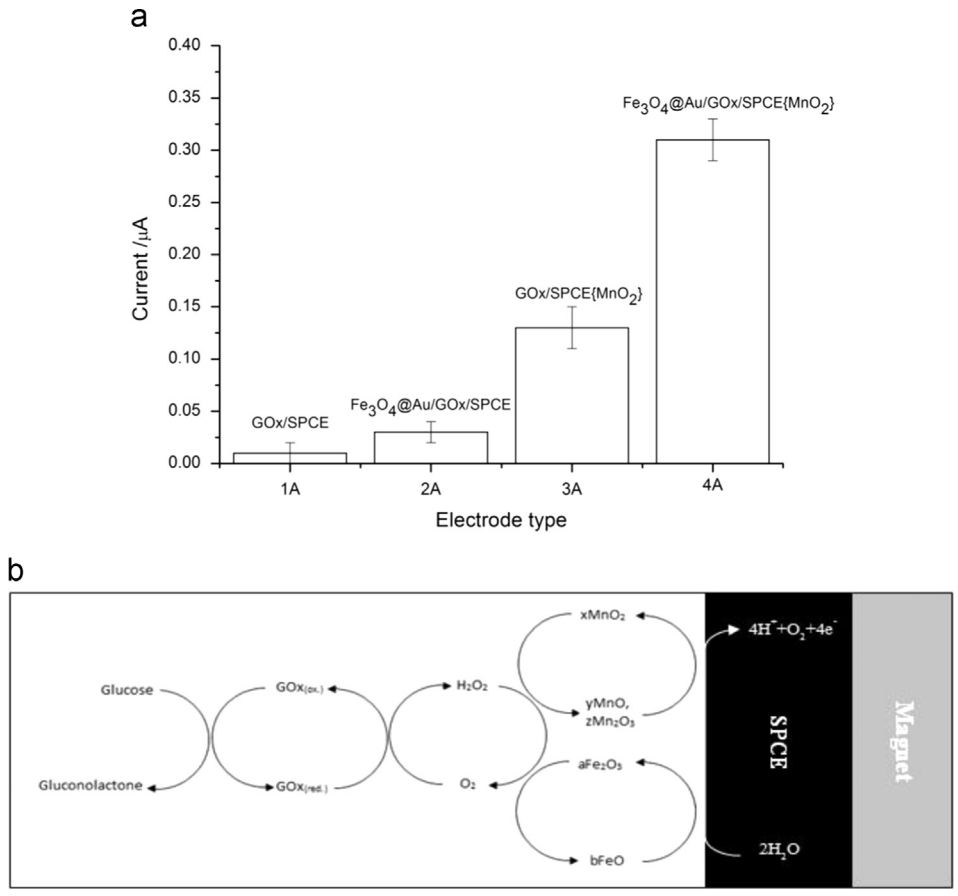

Fig. 3. Current responses of different electrodes for 0.5 mmol L^{-1} glucose solution (a) and proposed reaction mechanism for the detection of glucose with Fe_3O_4@Au/GOx/SPCE{MnO_2} (b).

containing the immobilized enzyme and MnO_2 in the bulk electrode material (4A).

From these studies it can be concluded that (i) Au seeds are attached to the magnetic core nanoparticles, (ii) the enzyme is immobilized on the nanoparticles, and (iii) MnO_2 as a modifier for SPCE improves the amperometric signal obtained with an applied potential of +0.38 V significantly.

Fig. 3b shows a sketch of the electrode reactions for the detection of glucose. From previous studies it is known that MnO_2 is reduced to lower oxidation states while H_2O_2 is oxidized to oxygen [35]. As can be seen in the comparison in Fig. 3 there seems to be a significant synergistic oxidative effect of Fe_3O_4 on H_2O_2. Iron oxides are known to act catalytically on the electrochemical oxidation and reduction of hydrogen peroxide but no mechanistic interpretation has been given so far [36]. We assume that the core of the nanoparticles, i.e., Fe_3O_4 ($=FeO \cdot Fe_2O_3$), participates in the oxidation of hydrogen peroxide probably via a Fenton-like process (Eq. (1)) [37,38].

$$Fe^{3+} + H_2O_2 \rightarrow Fe^{2+} + H^+ + HO_2. \quad (1)$$

The resulting Fe^{II} can be electrochemically oxidized to Fe^{III}, whereas the hydroperoxy radical HO_2· could be further oxidized to oxygen by MnO_2 explaining the synergistic effect.

3.2. Optimization of experimental parameters

3.2.1. Operating potential

The operating potential is a crucial parameter in hydrodynamic amperometry. In the present study the dependence of the applied potential on the MnO_2-modified SPCE with magnetically attached Fe_3O_4@Au/GOx exposed to a carrier solution was investigated. The modified SPCE showed high current responses with potentials higher than +0.2 up to +0.4 V; beyond this the signal remained steady (see Fig. 4a). In the case where MnO_2 alone acts as a catalyst, operating potentials of +0.4 V or higher should be expected [35]. Thus, we may conclude from this study that Fe_3O_4 works synergistically with MnO_2 to catalyze the oxidation of H_2O_2.

3.2.2. Effect of the pH of the buffer solution

The pH dependence of the biosensor was studied in 0.1 mol L^{-1} PBS within the range from 6.0 to 7.4. The optimum pH was evaluated as 7.0 (Fig. 4b) yielding maximum peak current. At higher pH values the current leveled off and below pH 7.0 the signal was sharply diminished to a pH value of 6.4 followed by a plateau between pH of 6.4 and 6.0. The optimum pH value found under the given experimental conditions corresponds well to the value reported by Khurshid et al. [39]. In their study glucose oxidase had a significant activity range from pH 4.0 to 7.0 similar to that found by Kalisz et al. [40] who reported the pH optimum in the slightly acidic to neutral range.

3.2.3. Enzyme loading

To study the effect of enzyme loading on the sensitivity of the biosensor different volumes (5–25 μL) of 25 U mL^{-1} GOx solution was mixed with 200 μL of the Fe_3O_4@Au seeds nanoparticles suspension (8×0^{14} particles mm^{-2}) in 300 μL total volume for all conditions and left to stand overnight. Optimum sensitivity was

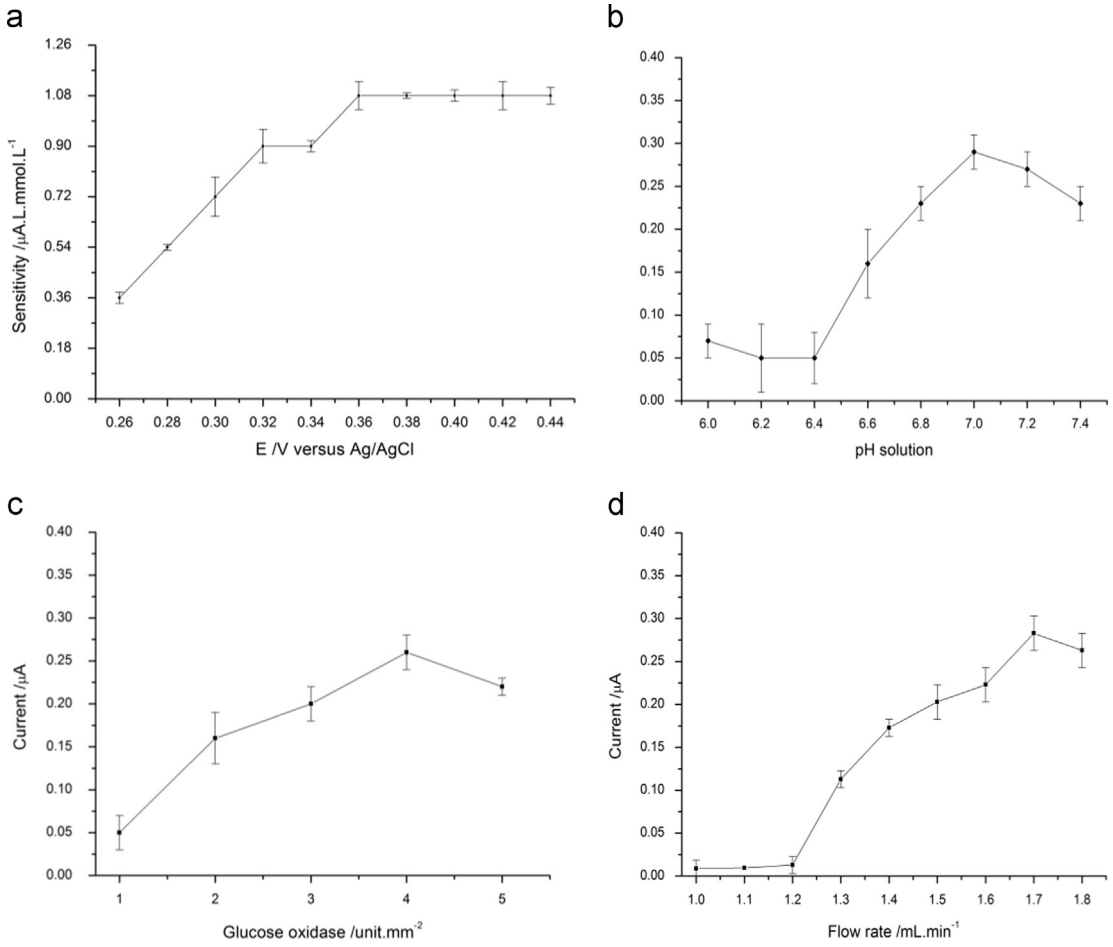

Fig. 4. Dependence of the current response in FIA mode on (a) the working potential, (b) the pH of the carrier solution, (c) the enzyme loading and (d) the flow rate of the carrier; carrier PBS 0.1 mol L^{-1}, pH 7.0; glucose concentration: 1 mmol L^{-1}; injection volume: 100 μL.

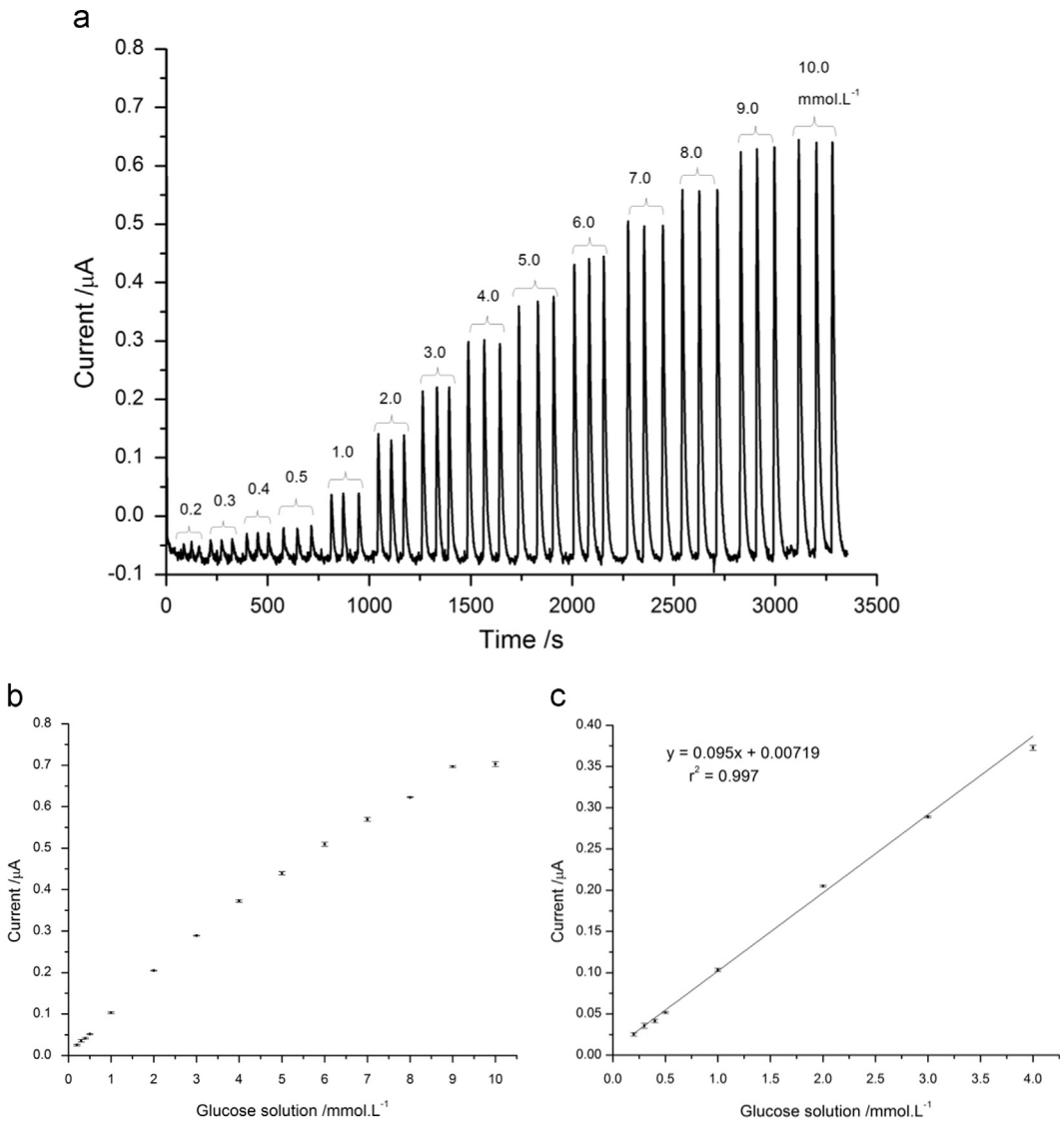

Fig. 5. (a) Typical response curve of the proposed glucose biosensor (0.2–10.0 mmol L^{-1} glucose solution) under optimal conditions: 0.1 mol L^{-1} PBS (pH 7.0); flow rate at 1.7 mL min^{-1}, working potential: +0.36 V; (b, c) calibration plots.

Table 1
Glucose concentration in different samples obtained by the biosensor and a comparative method.

Sample	Glucose content (%, m/m)			t_{calc}	t_{crit} (0.95)	Relative difference (%)
	Nominal	Biosensor (Mean ± SD)	Glucose meter (Mean ± SD)			
Glucose sirup	50	50.4 ± 0.7	49.7 ± 0.3	1.592	2.920	+1.4
Honey #1	–	28.8 ± 0.8	30.2 ± 0.7	2.281	2.920	−4.6
Honey #2	–	37.4 ± 0.8	39.2 ± 0.8	2.756	2.920	−4.6
Energy drink	5.0	5.0 ± 0.7	4.9 ± 0.8	0.163	2.920	+2.0

$n=3$ Measurements.

obtained when using 20 μL of GOx solution (3.89 unit mm^{-2}) as illustrated in Fig. 4c.

3.2.4. *Effect of flow rate*

The flow rate plays an important role for shape, height and area of analytical signals.

A higher flow rate usually means a decrease in signal due to a shorter time frame of reaction between the modifiers and the analyte. However, increasing flow rates causes diminishing of the dispersion of the analyte and decrease of the Prandtl and the diffusion layers at the electrode surface which should lead to an increase of the diffusion current [35]. Under the experimental conditions in this study (Fig. 4d) slow flow rates < 1.2 mL min^{-1} produced only small signals. Probably the thickness of the diffusion layer allows only outer lying enzyme molecules to react with the analyte, combined with a longer residence time of hydrogen peroxide in the diffusion layer which favors the chemical decomposition of the intermediate in the iron oxide. With increased flow rates the diffusion layer becomes thinner, more enzyme molecules are involved and the diffusion time becomes shorter. An optimum of 1.7 mL min^{-1} was found in the setup used in this study. This value was subsequently applied to the amperometric determination of

Table 2
Comparison of various glucose biosensors based on modified electrode.

Modified electrode	Electrode type	Detection method	Sensing element	Method of enzyme immobilization	LOD	Linear range	Sensitivity	Ref.
Fe_3O_4@SiO_2/MWNTs	GCE	Amperometry	Gox	Chemisorption and covalent bonding	0.8 μM	1 μM–30 mM	58.9 μA mM^{-1} cm^{-2}	[41]
ZnO nanorods/Au	GCE	Amperometry	Gox	Entrapment	0.01 μM	0.1–33 μM	1492 μA mM^{-1} cm^{-2}	[42]
PMMA–BSA	GCE	Amperometry	GOx	Entrapment	–	0.2–9.1 mM	44.1 μA mM^{-1} cm^{-2}	[43]
Au@Ag shell nanorods	GCE	Amperometry	GOx	Physical adsorption	0.67 μM	0.02–7.02 mM	33.67 μA mM^{-1} cm^{-2}	[44]
Conducting polymer	GCE	Amperometry	PyOx	Entrapment	0.33 μM	0.02–0.5 mM	0.006 μA mM^{-1} cm^{-2}	[45]
Nf /Au–Fe_3O_4@SiO_2	ITO Magnetism-electrode	EIS, Amperometry	GOx/HRP	Chemisorption	10 μM	0.05–1.0 mM and 1–8 mM	92.14 and 15.00 μA mM^{-1} cm^{-2}	[46]
Au–PDA–Fe_3O_4	MGCE	Amperometry	GOx	Entrapment	6.5 μM	0.02–1.875 mM	–	[47]
Fe_3O_4–enzyme–Ppy	MGCE	Potentiometry	GOx	Covalent bonding	0.3 μM	0.5 μM–34 mM	–	[48]
Fe_3O_4–RGO	MGCE	Amperometry	GOx	Chemisorption	0.15 μM	0.05–1.5 mM	9.04 μA mM^{-1} cm^{-2}	[49]
Fe_3O_4/Cs/Nf	Pt	Amperometry	GOx	Entrapment	6 μ M	6 μM–2.2 mM	11.54 μA mM^{-1} cm^{-2}	[50]
Os-complex	SPCE	Amperometry	GOx	Microencapsulation	30 μM	0.1–10 mM	–	[51]
MnO_2	SPCE	Amperometry	GOx	Mixing with carbon matrix	1 μM	11 μM–13.9 mM	–	[24]
Ferri–Cos	SPCE	Amperometry	GOx	Covalent bonding	1.38 mM	up to 33.3 mM	0.677 μA mM^{-1}	[52]
Fe_3O_4@Au/ MnO_2	SPCE	Amperometry	GOx	Chemisorption	13.2 μM	200 μM–9.0 mM	2.52 μA mM^{-1} cm^{-2}	Present work

Abbreviations: MWNTs, multiwall carbon nanotubes; PMMA–BSA, poly(methyl methacrylate)–bovine serum albumin; Nf, Nafion; PDA, polydopamine; Ppy, Polypyrrole, RGO, reduced graphene oxide; Cs, chitosan; Ferri–COs, ferricyanide–chitosan oligomers; GCE, glassy carbon electrode; PyOx, pyranose oxidase, ITO, indium tin oxide; MGCE, magnetic glassy carbon electrode, Pt, platinum; SPCE, screen printed carbon electrode; GOx, glucose oxidase; HRP, Horseradish peroxidase; EIS, electrochemical impedance spectroscopy

glucose. Flow rates higher than 1.7 mL min^{-1} resulted again in decrease of the response, probably because of entering a time domain where the enzyme kinetics wasalready dominating.

3.3. Calibration

The relationship between the amperometric peak current and the concentration of glucose (under optimal working conditions are as follows: operational potential, +0.38 V vs. Ag/AgCl; pH of phosphate buffer, 7.0; flow rate, 1.7 mL min^{-1}) in the range from 0.2 to 9.0 mmol L^{-1} is depicted in Fig. 5. The detection limit (3SD.) was determined as 0.013 mmol L^{-1}, and the limit of quantification as 0.3 mmol L^{-1}. A practical linear relation between signal and glucose concentration was found to be in the range 0.2–4.0 mmol L^{-1}.

3.4. Reproducibility, repeatability and stability of the biosensor

The electrode-to-electrode reproducibility was estimated from the current response to 1 mmol L^{-1} glucose of three biosensors. A mean current response of 0.35 μA was acquired with a RSD of 4.0%. The repeatability of one electrode was enumerated with 1 mmol L^{-1} glucose yielding a RSD of 2.8% for ten successive measurements. When the biosensor was stored at 4 °C, it retained 90% of its initial current response for glucose after repeated use for over one week, and 80% after one month.

3.5. Interferences

Interferences which may contain in biological sample such as acetic acid, ascorbic acid and citric acid were investigated. These possible interfering substances were evaluated in a molar ratio to glucose of 1:1 and 10:1 under the optimized conditions for the determination of glucose. The experiments were performed as mixed solutions in phosphate buffer and the current signals were compared with the response current from pure glucose. Only ascorbic acid at molar concentration ratios 10:1 or higher with respect to glucose interfered notably with an increase of the signal (around 30% for 10:1 mol:mol) while the others showed effects within the experimental uncertainty.

3.6. Quantification of glucose in honey samples

The developed biosensor was used to determine glucose in glucose sirup, honey samples and in an energy drink; these matrices contain ascorbic acid in concentrations, where they do not significantly interfere; investigations for samples with higher concentrations of the interferent are currently in progress. The glucose determinations were done by FIA measurements under optimized conditions using the standard addition method. The results were compared with a calibrated commercial glucose meter as shown in Table 1. The validity of the method was checked by recovery determinations. The relative differences between both methods ranged from 1.4% to 4.6% with respect to the reference determination and are in good agreement. Applying the paired *t*-test, the *t*-value is significantly smaller than the tabulated critical value (2.92 for $\alpha = 0.05$) at a degree of freedom of 2, indicating that there is no significant statistical difference between these results at a confidence interval for 95% probability. The results indicated also that there are no significant matrix interferences in the analyzed samples as well as that the proposed method is sufficiently accurate and suitable for the quantification of glucose in the mentioned samples.

Table 2 summarizes a short overview of the characteristics of the new method presented here compared to other methods from the literature. The advantages of the current one are a wide linear

range combined with a simple way of preparation and handling of the biosensor. The limit of detection is higher than with some other methods but still satisfying for most applications dealing with the determination of glucose.

4. Conclusions

This work presents a screen printed glucose biosensor produced by immobilizing glucose oxidase via direct chemisorption on gold seeds generated on magnetite nanoparticles. The resulting nanoparticles were immobilized on the surface of a MnO_2-modified screen-printed carbon electrode exploiting synergistic catalytic detection of hydrogen peroxide by both metal oxides involved. Thus, the proposed procedure enables simple preparation of modified screen-printed electrode and exhibits reliability, high sensitivity and stability using flow-injection analysis. On the basis of these results, this biosensor might be applied in the quantification of the glucose content in food samples.

Acknowledgements

The authors acknowledge scholarship support from the Department of Chemistry, Faculty of Science, UbonRatchathani University (Thailand), the Commission on Higher Education, the Center of Excellence for Innovation in Chemistry (PERCH-CIC), the Thailand Research Fund (TRF Grant no. RDG5750100), and the financial assistance from AseaUniNet.

References

[1] B.D. Malhotra, A. Chaubey, Sens. Actuators B 91 (2003) 117.
[2] P. D'Orazio, Clin. Chim. Acta 334 (2003) 4.
[3] S. Borgmann, A. Schulte, S. Neugebauer, W. Schuhmann, in: R.C. Alkire, D.M. Kolb, J. Lipkowski (Eds.), Bioelectrochemistry: Fundamentals, Applications and Recent Developments, WILEY-VCH Verlag GmbH & Co. KGaA, Weinheim, Germany, 2011, pp. 1–83.
[4] M. Moyo, J.O. Okonkwo, N.M. Agyei, Enzym. Microb. Technol. 56 (2014) 28.
[5] R. Rawal, S. Chawla, Devender, C.S. Pundir, Enzym. Microb. Technol. 51 (2012) 179.
[6] A. Guerrieri, T.R.I. Cataldi, R. Ciriello, Sens. Actuators B 126 (2007) 424.
[7] S.B. Bankar, M.V. Bule, R.S. Singhal, L. Ananthanarayan, Biotechnol. Adv. 27 (2009) 489.
[8] M.C. Tsai, Y.C. Tsai, Sens. Actuators B 141 (2009) 592.
[9] T. Zhang, X.L. Xua, Y.N. Jin, J. Wu, Z.K. Xub, J. Mol. Catal. B: Enzym. 106 (2014) 56.
[10] Y. Zhang, D. Rochefort, Process Biochem. 46 (2011) 993.
[11] Q. Xin, Y. Jiang, J. Gao, L. Zhou, L. Ma, Y. He, F. Jia, Chin. J. Catal. 34 (2013) 1627.
[12] J. Wang, D. Leech, M. Ozsoz, S. Martinez, M.R. Smyth, Anal. Chim. Acta 245 (1991) 139.
[13] S.M. Reddy, P. Vadgama, Anal. Chim. Acta 461 (2002) 57.
[14] L. Su, X. Qiu, L. Guo, F. Zhang, C. Tung, Sens. Actuators B 99 (2004) 499.
[15] R. Nenkova, D. Ivanova, J. Vladimirova, T. Godjevargova, Sens. Actuators B 148 (2010) 59.
[16] E. Katz, O. Lioubashevski, I. Willner, J. Am. Chem. Soc. 127 (2005) 3979.
[17] J. Shim, G.Y. Kim, S.H. Moon, J. Electroanal. Chem. 653 (2011) 14.
[18] G.K. Kouassi, J. Irudayaraj, Anal. Chem. 78 (2006) 3234.
[19] L.L. Pang, J.S. Li, J.H. Jiang, Y. Le, G.L. Shen, R.Q. Yu, Sens. Actuators B 127 (2007) 311.
[20] Y.R. Cui, C. Hong, Y.L. Zhou, Y. Li, X.M. Gao, X.X. Zhang, Talanta 85 (2011) 1246.
[21] J. Baniukevic, I. HakkiBoyaci, A. GoktugBozkurt, U. Tamer, A. Ramanavicius, A. Ramanaviciene, Biosens. Bioelectron. 43 (2013) 281.
[22] U. Tamer, Y. Gundogdu, I.H. Boyacı, K. Pekmez, J. Nanopart. Res. 12 (2010) 1187.
[23] N.W. Beyene, P. Kotzian, K. Schachl, H. Alemu, E. Turkusic, A. Copra, H. Moderegger, I. Svancara, K. Vytras, K. Kalcher, Talanta 64 (2004) 1151.
[24] E. Turkusic, J. Kalcher, E. Kahrovic, N.W. Beyene, H. Moderegger, E. Sofic, S. Begic, K. Kalcher, Talanta 65 (2005) 559.
[25] J. Yu, T. Zhao, B. Zeng, Electrochem. Commun. 10 (2008) 1318.
[26] Y. Xin, X. Fu-Bing, L. Hong-Wei, W. Feng, C. Di-Zhao, W. Zhao-Yang, Electrochim. Acta 109 (2013) 750.
[27] A.G. El-Deen, N.A.M. Barakat, H.Y. Kim, Desalination 344 (2014) 289.
[28] P. Fanjul-Bolado, P.J. Lamas-Ardisana, D. Hernández-Santos, A. Costa-García, Anal. Chim. Acta 638 (2009) 133.
[29] Q. Gao, Y. Guo, W. Zhang, H. Qi, C. Zhang, Sens. Actuators B 153 (2011) 219.
[30] T.F. Tormin, R.R. Cunha, R.A.B. da Silva, R.A.A. Munoz, E.M. Richter, Sens. Actuators B 202 (2014) 93.
[31] G.K. Kouassi, J. Irudayaraj, Anal. Chem. 78 (2006) 3234.
[32] U. Tamer, Y. Gundogdu, I. Hakkı Boyacı, K. Pekmez, J. Nanopart. Res. 12 (2010) 1187.
[33] B. Kalska-Szostko, M. Rogowska, A. Dubis, K. Szyman´ ski, Appl. Surf. Sci. 258 (2012) 2783.
[34] X. Chen, J. Zhu, Z. Chen, C. Xu, Y. Wang, C. Yao, Sens. Actuators B 159 (2011) 220.
[35] K. Schachl, H. Alemu, K. Kalcher, J. Jezkova, I. Svancara, K. Vytras, Analyst 122 (1997) 985.
[36] H. Zhao, Y. Wang, Y. Wang, T. Cao, G. Zhao, Appl. Catal. B 125 (2012) 120.
[37] C. Jiang, Z. Gao, H. Qu, J. Li, X. Wang, P. Li, H. Liu, J. Hazard. Mater. 250–251 (2013) 76.
[38] A. Bach, H. Shemer, R. Semiat, Desalination 264 (2010) 188.
[39] S. Khurshid, M.A. Kashmiri, Z. Quershi, W. Ahmad, Afr. J. Biotechnol. 10 (2011) 1674.
[40] H.M. Kalisz, H.J. Hecht, D. Schomburg, R.D. Schmid, Biochim. Biophys. Acta 1080 (2) (1991) 138.
[41] T.T. Baba, S. Ramaprabhu, Talanta 80 (2010) 2016.
[42] Y. Wei, Y. Li, X. Liu, Y. Xian, G. Shi, L. Jin, Biosens. Bioelectron. 26 (2010) 275.
[43] C. HeAuthor Vitae, J. LiuAuthor Vitae, Q. ZhangAuthor Vitae, C. Wu, Sens. Actuators B 166–167 (2012) 802.
[44] X. Yang, Y. Wang, Y. Liu, X. Jiang, Electrochim. Acta 108 (2013) 39.
[45] T.C. Gokoglan, S. Soylemez, M. Kesik, S. Toksabay, L. Toppare, Food Chem. 172 (2015) 219.
[46] X. ChenAuthor Vitae, J. ZhuAuthor Vitae, Z. ChenAuthor Vitae, C. XuAuthor Vitae, Y. WangAuthor Vitae, C. Yao, Sens. Actuators B 159 (2011) 220.
[47] H.P. Peng, R.P. Liang, L. Zhang, J.D. Qiu, Biosens. Bioelectron. 42 (2013) 293.
[48] Z. Yang, C. Zhang, J. Zhang, W. Bai, Biosens. Bioelectron. 51 (2014) 268.
[49] L. Yu, H. Wu, Z. Wang, H. Cao, C. Fu, N. Jia, Nanomicro Lett. 6 (2014) 258.
[50] L. Yang, X. Ren, F. Tang, L. Zhang, Biosens. Bioelectron. 25 (2009) 889.
[51] C. Zhang, Q. Gao, M. Aizawa, Anal. Chim. Acta 426 (2006) 33.
[52] S.H. Lee, H.Y. Fang, W.C. Chen, Sens. Actuators B 117 (2006) 236.